

PAPER

Theoretical study of the characteristics of a continuous wave iron-doped ZnSe laser

To cite this article: Qikun Pan *et al* 2018 *Laser Phys.* **28** 035002

View the [article online](#) for updates and enhancements.

Recent citations

- [A Gain-Switched Fe:ZnSe Laser Pumped by a Pulsed Ho,Pr:LLF Laser](#)
Ying-Yi Li *et al*

Theoretical study of the characteristics of a continuous wave iron-doped ZnSe laser

Qikun Pan^{1,2,3}, Fei Chen^{1,2}, Jijiang Xie^{1,2}, Chunrui Wang^{1,2}, Yang He^{1,2}, Deyang Yu^{1,2} and Kuo Zhang^{1,2}

¹ State Key Laboratory of Laser Interaction with Matter, Changchun Institute of Optics, Fine Mechanics and Physics, Chinese Academy of Sciences, 3888 Dongnanhu Road, Changchun 130033, People's Republic of China

² Innovation Laboratory of Electro-Optical Countermeasures Technology, Changchun Institute of Optics, Fine Mechanics and Physics, Chinese Academy of Sciences, 3888 Dongnanhu Road, Changchun 130033, People's Republic of China

E-mail: panqikun2005@163.com

Received 10 August 2017, revised 28 November 2017

Accepted for publication 30 December 2017

Published 8 February 2018



Abstract

A theoretical model describing the dynamic process of a continuous-wave $\text{Fe}^{2+}:\text{ZnSe}$ laser is presented. The influence of some of the operating parameters on the output characteristics of an $\text{Fe}^{2+}:\text{ZnSe}$ laser is studied in detail. The results indicate that the temperature rise of the $\text{Fe}^{2+}:\text{ZnSe}$ crystal is significant with the use of a high power pump laser, especially for a high doped concentration of crystal. The optimal crystal length increases with decreasing the doped concentration of crystal, so an $\text{Fe}^{2+}:\text{ZnSe}$ crystal with simultaneous doping during growth is an attractive choice, which usually has a low doped concentration and long length. The laser pumping threshold is almost stable at low temperatures, but increases exponentially with a working temperature in the range of 180 K to room temperature. The main reason for this phenomenon is the short upper level lifetime and serious thermal temperature rise when the working temperature is higher than 180 K. The calculated optimum output mirror transmittance is about 35% and the performance of a continuous-wave $\text{Fe}^{2+}:\text{ZnSe}$ laser is more efficient at a lower operating temperature.

Keywords: $\text{Fe}^{2+}:\text{ZnSe}$ laser, continuous-wave, theoretical model, operating temperature, output characteristics

(Some figures may appear in colour only in the online journal)

1. Introduction

Mid-infrared lasers have attracted much attention for wide applications such as eye-safe laser radar, trace gas analysis, environmental monitoring, spectroscopy, laser communication, and numerous military applications. The transition metal iron doped ZnSe ($\text{Fe}^{2+}:\text{ZnSe}$) laser has a broad absorption spectrum (helpful for broadband pumping) and broad fluorescence spectrum (helpful for broadband tuning), which is an innovative solid state laser in the mid-infrared range of 4–4.5 μm [1–3].

In recent years, solid state $\text{Fe}^{2+}:\text{ZnSe}$ lasers excited by a high power flash-lamp-pumped Er:YAG laser and a high-energy non-chain pulsed HF/DF laser have developed rapidly

[4–10]. In 2015, using a 15 J flash-lamp-pumped Er:YAG laser as the excitation source, Velikanov demonstrated an $\text{Fe}^{2+}:\text{ZnSe}$ laser with a 4.9 J single pulse energy at 85 K, with a laser slope efficiency of 51% [4]. Later, Velikanov replaced the excitation source with a non-chain pulsed HF laser and obtained an $\text{Fe}^{2+}:\text{ZnSe}$ laser with a pulse energy of 1.2 J at room temperature [5]. Also in 2015, Martyshkin reported a repetition rate $\text{Fe}^{2+}:\text{ZnSe}$ laser with a maximum average power of 35 W at 77 K [6]. Both the flash-lamp-pumped Er:YAG laser and the non-chain pulsed HF/DF laser pump source have the disadvantages of large volume and low wall-plug efficiency [11, 12]. However, solid state continuous-wave $\text{Fe}^{2+}:\text{ZnSe}$ lasers using an LD pumped Er:YAG laser as the excitation source have the advantages of compact size and high wall-plug efficiency, which would have prospects in the future.

³ Author to whom any correspondence should be addressed.

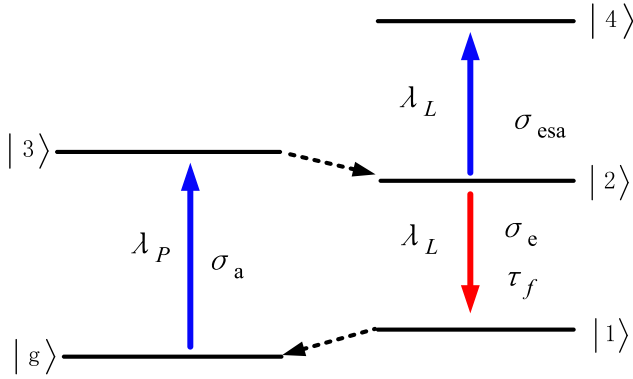


Figure 1. Energy level diagram of an $\text{Fe}^{2+}:\text{ZnSe}$ gain medium.

Sennaroglu reported a theoretical model of a continuous-wave $\text{Cr}^{2+}:\text{ZnSe}$ laser, and the output power performance was accurately simulated by the model [13]. There are some similarities between the energy level structure and the radiation mechanism of $\text{Fe}^{2+}:\text{ZnSe}$ and $\text{Cr}^{2+}:\text{ZnSe}$ lasers. The influence of the temperature rise on the fluorescence lifetime of a $\text{Cr}^{2+}:\text{ZnSe}$ laser is small with a low power pump, so the temperature factor is neglected in Sennaroglu's model [13]. However, the case of the $\text{Fe}^{2+}:\text{ZnSe}$ laser is different, as the temperature rise has a significant impact on fluorescence lifetime [3]. In this paper, taking into account the influence of the temperature rise caused by the laser pump on the fluorescence lifetime of an $\text{Fe}^{2+}:\text{ZnSe}$ laser, the theoretical model that can describe the laser dynamic process of a continuous-wave $\text{Fe}^{2+}:\text{ZnSe}$ laser is presented. The influence of temperature rise of crystal, crystal length, doped concentration of crystal, and output mirror transmittance on the performance of an $\text{Fe}^{2+}:\text{ZnSe}$ laser is studied by this model. The simulated output power of a continuous-wave $\text{Fe}^{2+}:\text{ZnSe}$ laser is consistent with the experimental result reported by Evans [14].

2. Model of continuous-wave $\text{Fe}^{2+}:\text{ZnSe}$ laser

The modified four-level energy diagram used in the model of the continuous-wave $\text{Fe}^{2+}:\text{ZnSe}$ laser is shown in figure 1. Pump photons at wavelength λ_p are absorbed by Fe^{2+} ions which then are excited from the ground state $|g\rangle$ to the first excited state $|3\rangle$. The energy level lifetime of $|3\rangle$ is much shorter than the upper level $|2\rangle$. Decay from $|3\rangle$ to $|2\rangle$ is assumed to occur very rapidly, leaving approximately no ions on level $|3\rangle$ in the steady state. Ions on level $|2\rangle$ can either come down to $|1\rangle$ by stimulated and spontaneous emission or get promoted to the higher energy level $|4\rangle$ as result of excited-state absorption. Finally, the rapid decay from $|1\rangle$ to $|g\rangle$ can be assumed as leaving level $|1\rangle$ empty.

The absorption and the emission bands of the $\text{Fe}^{2+}:\text{ZnSe}$ laser overlap in the 3.5–5 μm spectral range at room temperature [15], so some laser photons at wavelength λ_l are absorbed by ground-state Fe^{2+} ions which are excited to the upper level $|2\rangle$. For the short fluorescence lifetime of Fe^{2+} ions at room temperature, the Fe^{2+} ions on the upper level come down to the lower level and radiate laser photons at wavelength λ_l

simultaneously. During this process, the absorbed and radiated photons have the same wavelength, so the quantum efficiency is about 1. Therefore, the process of absorption from the ground state at laser wavelength λ_l is neglected in this model at room temperature. The temporal evolution of the ion density N_2 on upper level $|2\rangle$ can be described by the following rate equation:

$$\frac{dN_2(r, z)}{dt} = \frac{\sigma_a \lambda_p I_p(r, z)}{hc} N_g(r, z) - \frac{\sigma_e \lambda_l I_l(r, z)}{hc} N_2(r, z) - \frac{\sigma_{esa} \lambda_l I_l(r, z)}{hc} - \frac{N_2(r, z)}{\tau_f}. \quad (1)$$

Here, $N_g(r, z)$ is the ion density of ground state $|g\rangle$; $I_p(r, z)$ is the pump intensity; $I_l(r, z)$ ($I_l(r, z) = I_1^+(r, z) + I_1^-(r, z)$) is the total cavity laser intensity at λ_l ; h is the Planck constant; σ_a is the absorption cross-section at λ_p ; σ_e is the emission cross-section; σ_{esa} is the excited-state absorption cross-section at λ_l ; λ_p and λ_l are the pump and laser wavelengths, respectively, and τ_f is the fluorescence lifetime, which is a function of temperature.

We assume that the decay from level $|4\rangle$ to $|2\rangle$ occurs very rapidly so that N_4 is negligible in the steady state. Hence, to a very good approximation, $dN_2/dt = -dN_g/dt$ and $N_t = N_g(r, z) + N_2(r, z)$. Under these approximations, it can be shown that in the steady state, the expression of N_2 becomes:

$$N_2(r, z) = N_t \frac{I_p(r, z)/I_{sa}}{1 + (1 + f)I_l(r, z)/I_{se} + I_p(r, z)/I_{sa}}, \quad (2)$$

where f ($f = \sigma_{esa}/\sigma_e$) is the normalized excited-state absorption strength at the laser wavelength λ_l . I_{sa} ($I_{sa} = hc/\sigma_a \lambda_p \tau_f$) and I_{se} ($I_{se} = hc/\sigma_e \lambda_l \tau_f$) are the absorption and emission saturation intensities, respectively.

In the steady state, stimulated absorption from the ground state leads to the attenuation of pump intensity, while stimulated emission from the upper laser level amplifies the circulating laser intensity. The propagation of I_p , I_l in the resonator consisting of M_1 , M_2 is shown in figure 2.

In the crystal of $\text{Fe}^{2+}:\text{ZnSe}$, under the condition of ignoring the atmospheric absorption of the pump laser ($I_{p1} = I_{p0}$), the axial pump laser intensity I_p can be given by the differential equation:

$$\frac{dI_p}{dz} = I_p(z) \frac{-a_{p0}(1 + (1 + f)I_l(z)/I_{se})}{1 + [I_p(z)/I_{sa} + (1 + f)I_l(z)/I_{se}]}, \quad (3)$$

where a_{p0} ($a_{p0} = \sigma_a N_g$) is the small-signal differential absorption coefficient at the pump wavelength λ_p . Meanwhile, ignoring the atmospheric absorption and scattering of the laser, we assume that $I_{12}^- = I_{11}^-$, $I_{14}^- = I_{13}^-$, $I_{16}^+ = I_{15}^+ = R_1 I_{14}^+$, $I_{18}^+ = I_{17}^+$, $I_{11}^- = R_2 I_{18}^+$. Above R_1 , R_2 is the reflectance of the cavity mirrors. In the crystal of $\text{Fe}^{2+}:\text{ZnSe}$, the axial laser intensity I_l can be given by the differential equation:

$$\frac{dI_l^\pm}{dz} = I_l^\pm(z) \pm \left[\frac{g_t(1 - f)I_p(z)/I_{sa}}{I_p(z)/I_{sa} + (1 + f)I_l^\pm(z)/I_{se}} - a_{l0} \right], \quad (4)$$

where g_t ($g_t = \sigma_e N_t$) is the maximum extractable small-signal differential gain coefficient and a_{l0} is the small-signal

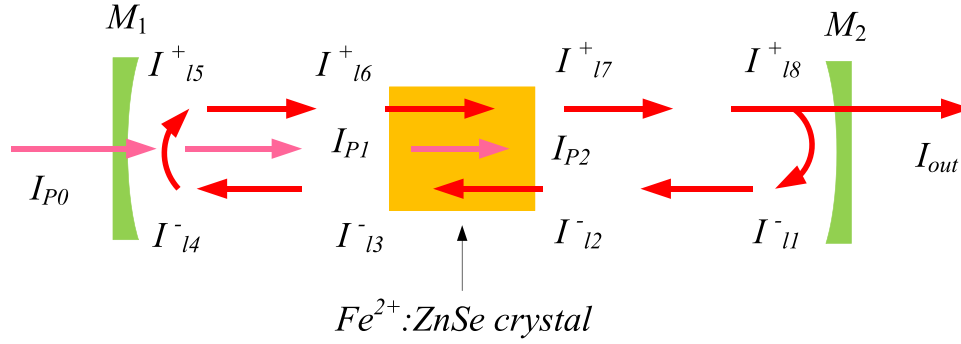


Figure 2. Schematic layout of laser propagation in the resonator.

differential absorption coefficient at the laser wavelength λ_l . By solving the above simultaneous equations, the laser intensity in the cavity can be obtained. Then, the output power can be calculated by $P_{out} = A(1 - R_2)I_{l8}^-$, where A is the laser cross-sectional area in the cavity.

Fedorov performed a least-squares fit of the lifetime data for an $\text{Fe}^{2+}:\text{ZnSe}$ crystal using the standard Mott model [16]:

$$\begin{aligned} \tau_f^{-1} &= \tau_{rad}^{-1} + \tau_{NR}^{-1} \\ \tau_{NR}^{-1} &= W_a \exp(-\Delta E_a/k_b T), \end{aligned} \quad (5)$$

where τ_{rad} and τ_{NR} are the radiative and non-radiative lifetimes, respectively; ΔE_a is the energy gap between the intersection of the adiabatic potentials of the ground and excited states and the minimum of adiabatic potential of the excited state; W_a is the relaxation parameter, and k_b is the Boltzmann's constant.

The effect of temperature on the cross-sections of absorption and emission are introduced in the model. The absorption cross-section spectra are obtained from absorption measurements [1], and different absorption cross-sections are used in the calculation. Emission cross-sections can be determined using the Fuchtbauer–Landenburg (FL) equation. Using the fundamental relationship between the spontaneous and stimulated processes, the FL equation can be written as:

$$\sigma_e = \frac{\lambda_l^5 I_l}{8\pi c n^2 \tau_{rad} \int I_l \lambda_l d\lambda_l}, \quad (6)$$

where n is the refractive index, and c is the speed of light.

The temperature of the crystal has a significant influence on the fluorescence lifetime, so the temperature rise of the crystal caused by the laser pump affects the output power of the $\text{Fe}^{2+}:\text{ZnSe}$ laser. By neglecting longitudinal heat conduction and by approximating the heat load as a square function, the temperature distribution $T_l(z)$ inside the crystal can be given by the following expression [13]:

$$T_l(z) = T_b + \frac{h_0(z)w_h(z)^2}{4\kappa} \left[1 + 2\ln\left(\frac{r_0}{w_h(z)}\right) \right]. \quad (7)$$

Here, T_b is the boundary temperature; r_0 is the effective crystal radius; and κ is the heat conductivity. The radial width $w_h(z)$ and the axial value $h_0(z)$ of the square heat load are further given by the following expressions:

$$w_h(z) = \frac{\omega_p(z)}{\sqrt{2}} \sqrt{\ln(1 + I_p(z)/I_{sa})} \quad (8)$$

$$h_0(z) = \frac{\eta_h a_{p0} I_p(z)}{1 + I_p(z)/I_{sa}}, \quad (9)$$

where $\omega_p(z)$ is the pump beam diameter and η_h is the heating coefficient. η_h gives the fraction of the absorbed pump energy that is converted to heat inside the crystal. Since the quantum efficiency of the $\text{Fe}^{2+}:\text{ZnSe}$ is near unity at a lower temperature, η_h is approximated as $(1 - \lambda_p/\lambda_l)$.

3. Simulation results and discussion

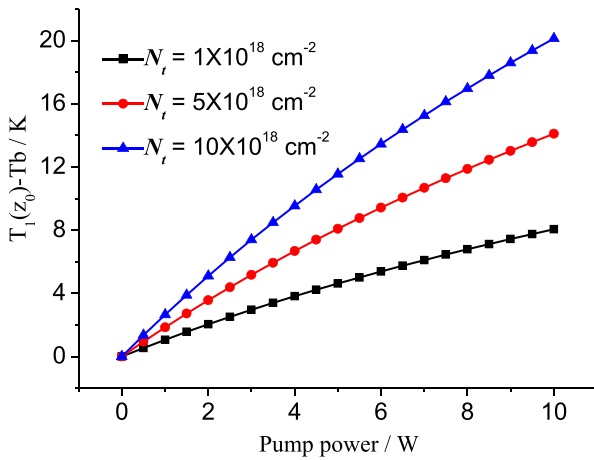
3.1. Temperature rise of the crystal

The working temperature of laser crystal influences the lifetime of the upper laser energy. Especially at room temperature, the lifetime of the upper laser energy will rapidly decrease with the rise in temperature [16]. The serious temperature rise of the crystal caused by the laser pump leads to a temperature quenching effect in the $\text{Fe}^{2+}:\text{ZnSe}$ laser. Before calculating the relationship between the output performance of the continuous wave $\text{Fe}^{2+}:\text{ZnSe}$ laser and the temperature of the crystal, the temperature rise caused by the laser pump is calculated using equation (7). The calculated variables are listed in table 1.

The absorption intensity of the pump laser is a function of the doped concentration of the $\text{Fe}^{2+}:\text{ZnSe}$ crystal. The relationship between the temperature rise at the incidence face of the crystal and the pump power is calculated at a doped concentration of $1 \times 10^{18} \text{ cm}^{-2}$, $5 \times 10^{18} \text{ cm}^{-2}$, and $10 \times 10^{18} \text{ cm}^{-2}$, respectively, and the results are shown in figure 3. The temperature at the incidence face increases linearly with the rise in pump power, and the higher the doped concentration, the higher the temperature rise of the crystal. The axial temperature rise at the maximum incident pump power of 10 W is approximately 20 K and 8 K with doped concentrations of $10 \times 10^{18} \text{ cm}^{-2}$ and $1 \times 10^{18} \text{ cm}^{-2}$, respectively. The experimental results of the lifetime temperature in [16] shows that the fluorescence lifetime deviates by less than 5% with the temperature rise of 20 K when the working temperature changes from 77–180 K. Since this deviation is very small, the influence of temperature on fluorescence lifetime is neglected in modeling the power performance of the continuous-wave in the temperature range of 77–180 K. When the working temperature is higher than 180 K, the fluorescence lifetime deviates by approximately 100% with a temperature rise of

Table 1. Values of the parameters of the Fe²⁺:ZnSe laser.

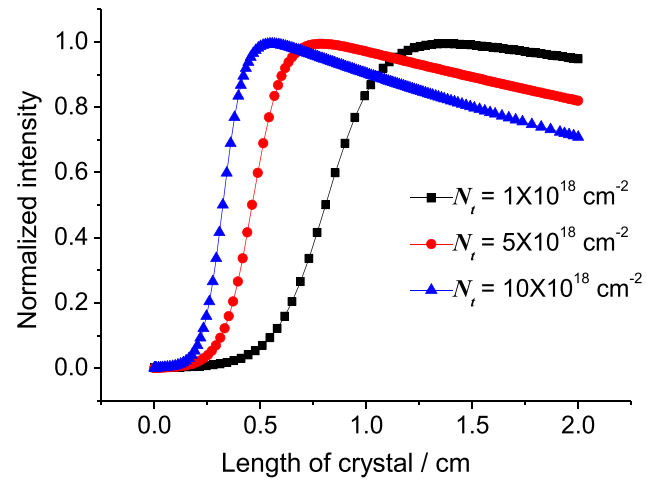
Definition	Parameter	Value/units
Energy gap	ΔE_a	1900 cm ⁻¹ [16]
Relaxation parameter	$1/W_a$	5 ns [16]
Normalized excited-state absorption strength	σ_{esa}/σ_e	0.17 [17]
Absorption cross-section	σ_a	1.3 × 10 ⁻¹⁸ cm ² at lower temperature [1] 0.97 × 10 ⁻¹⁸ cm ² at room temperature [1]
Wavelength of pump beam	λ_p	2.94 μm
Pump beam waist	ω	0.3 mm
Wavelength of laser beam	λ_l	4.1 μm
Heat conductivity	κ	0.19 W cm ⁻¹ K ⁻¹ [17]
Absorption coefficient	a_{l0}	0.1 cm ⁻¹
Doped concentration	N_t	5 × 10 ¹⁸ cm ⁻²
Refractive index	n	2.4
Crystal radius	R_0	3 mm

**Figure 3.** Calculated variation of the average axial temperature rise $T_l(z_0) - T_b$ as a function of the incident pump power.

20 K, so the influence of temperature on fluorescence lifetime cannot be neglected under this condition.

3.2. Laser threshold

After injecting the pump laser into the Fe²⁺:ZnSe crystal, and benefiting from the four-level energy structure, the population conversion between the upper and lower energy levels can be easily obtained. The laser grows due to the effect of the laser gain (stimulated amplification). Meanwhile, the laser weakens due to the effect of the loss (absorption loss and output coupling loss). Finally, whether the laser can be propagated or not depends on the values of gain and loss. Using the parameters listed in table 1, by solving equations (3) and (4), the relationship between laser intensity and crystal length in the cavity is calculated with different doping concentrations, and the results are shown in figure 4. Firstly, the laser intensity rapidly rises with the increment of crystal length and reaches the maximum. Then, for the weakening of the pump intensity and absorption loss at the longer crystal end, the laser intensity reduces gradually. The results show that the optical crystal length is about 13.6 mm, 7.9 mm, and 5.1 mm with a

**Figure 4.** Laser intensity as a function of crystal length at different doped concentrations.

doped concentration of 1×10^{18} cm⁻², 5×10^{18} cm⁻², and 10×10^{18} cm⁻², respectively. Taking into account the fact that the crystal with low doped concentration has a high temperature rise, an Fe²⁺:ZnSe single-crystal with simultaneous doping during growth is an attractive choice, which usually has a low doped concentration and long length.

Taking into account the influence of the temperature rise caused by the pump laser on the level lifetime of the Fe²⁺:ZnSe laser, the relationship between the laser threshold and the temperature of the crystal is calculated at different doping concentrations. During the calculation, the crystal length is set at an optimal value at each doping concentration. The calculation is shown in figure 5. When the temperature is lower than 180 K, the laser threshold (about 0.2 W) is invariable at each doping concentration, which is in agreement with the experimental results reported by Evans [14]. When the temperature is higher than 180 K, the temperature has an obvious influence on the threshold of the Fe²⁺:ZnSe laser and the laser threshold increases exponentially with the rise in the working temperature. Under the condition of the same pump power, the higher the doped concentration, the higher the laser threshold. At room temperature, the calculated laser threshold is about 20 W,

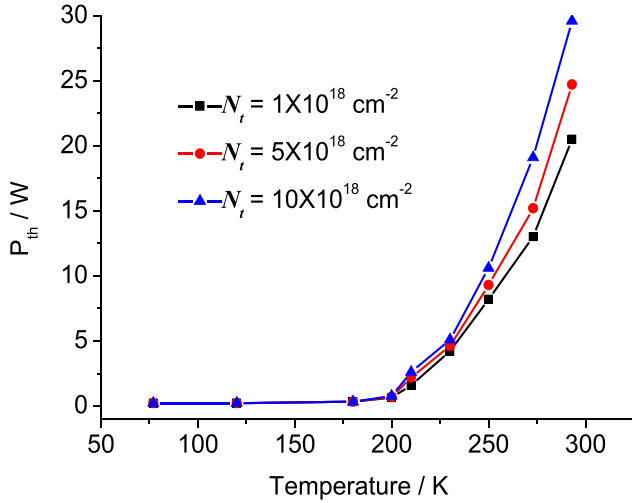


Figure 5. Laser threshold as a function of temperature at different doped concentrations.

24 W, and 29 W with doped concentrations of $1 \times 10^{18} \text{ cm}^{-2}$, $5 \times 10^{18} \text{ cm}^{-2}$, and $10 \times 10^{18} \text{ cm}^{-2}$, respectively.

3.3. Output characteristics of the continuous wave $\text{Fe}^{2+}:\text{ZnSe}$ laser

Under continuous wave pumping, the population of the upper level is invariable with the combined effect of stimulated absorption and emission, so the continuous wave $\text{Fe}^{2+}:\text{ZnSe}$ laser has a stable output power. By simultaneously solving equations (2)–(4), using the parameters listed in table 1, the relationship between the laser output power and the pump power is calculated, and the results are shown in figure 6. When the temperature is 77 K, ignoring the influence of the temperature rise on the level lifetime, the output power of the $\text{Fe}^{2+}:\text{ZnSe}$ laser increases linearly with the pump power, and the laser slope efficiency is about 42%. This simulation is in good agreement with the experiment reported by Evans [14], which shows that the model can be used to analyze the laser dynamic process of a continuous-wave $\text{Fe}^{2+}:\text{ZnSe}$ laser. By using thermoelectric coolers, a lower working temperature can easily reach 233 K, where the influence of the temperature rise on the level lifetime should not be ignored. The output power of the $\text{Fe}^{2+}:\text{ZnSe}$ laser increases with pump power, but the laser slope efficiency drops to 25%. And the laser efficiency further drops when the pump power is higher than 9 W. At room temperature, it is hard to operate a continuous-wave $\text{Fe}^{2+}:\text{ZnSe}$ laser. Now, scaling up the output power of the continuous-wave $\text{Fe}^{2+}:\text{ZnSe}$ laser is limited by the pump laser power at a lower temperature. While short level lifetime and serious thermal temperature rise are the key factors in limiting the operation of the $\text{Fe}^{2+}:\text{ZnSe}$ laser operation at room temperature.

In order to determine the optimal transmittance of the output mirror, the above procedure is repeated as a function of output mirror transmittance. At a temperature of 77 K and a pump power of 2 W, the relationships among the laser power, optical efficiency and transmittance of output mirror are calculated,

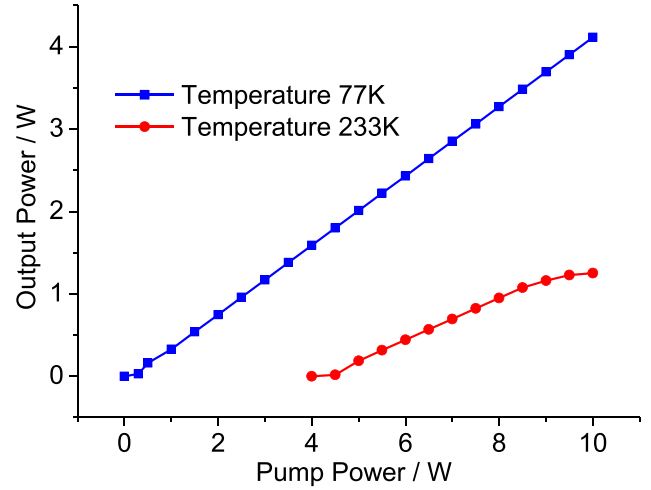


Figure 6. $\text{Fe}^{2+}:\text{ZnSe}$ laser output power as a function of pump power at temperature of 77 K and 233 K.

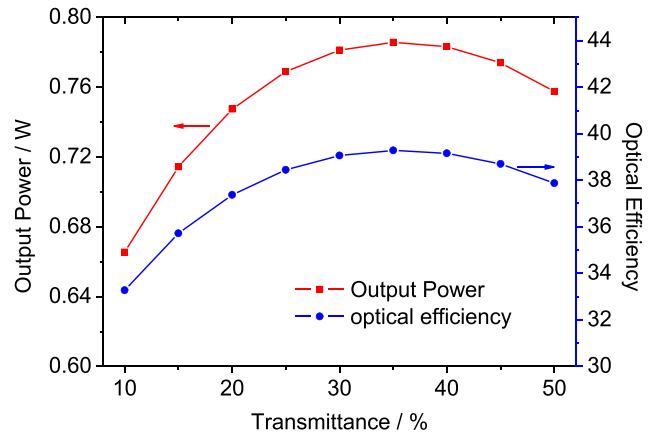


Figure 7. $\text{Fe}^{2+}:\text{ZnSe}$ laser output power and optical efficiency as a function of transmittance.

and the results are shown in figure 7. The laser power, optical efficiency, and transmittance of the output mirror are in a quadratic curve. The optimal transmittance is about 35%, and the maximum laser power and optical efficiencies are 0.78 W and 39%, respectively.

4. Conclusion

A theoretical model has been built to study the characteristics of a continuous wave $\text{Fe}^{2+}:\text{ZnSe}$ laser, and the temperature rise of crystal caused by a pump laser is calculated. Under the temperature range of 77 K–180 K, with an optimal crystal length, the doped concentration and the temperature rise have little effect on the output performance of the $\text{Fe}^{2+}:\text{ZnSe}$ laser. The laser threshold is about 0.2 W, and the laser slope efficiency is about 42% at 77 K, which is the optimal working temperature for a continuous-wave $\text{Fe}^{2+}:\text{ZnSe}$ laser. When the temperature is higher than 180 K, the doped concentration and the temperature rise have an obvious impact on the output performance of the $\text{Fe}^{2+}:\text{ZnSe}$ laser. At 233 K, which can be easily reached by using thermoelectric coolers, the laser

threshold and laser slope efficiency are about 4.5 W and 25%, respectively. At room temperature, it is hard to operate the continuous-wave $\text{Fe}^{2+}:\text{ZnSe}$ laser due to its high laser threshold and serious thermal temperature rise.

Acknowledgments

This work is supported by the International Cooperation Special Fund from Ministry of Science and Technology, PRC (2016YFE0120200), the National Natural Science Foundation of China (61705219), the Key Science and Technology Project Bidding of Jilin Province (20160203016GX), and the Science and Technology Innovation Talents Project of Jilin Province (20170519012JH).

References

- [1] Adams J J *et al* 1999 4.0–4.5 μm lasing of $\text{Fe}:\text{ZnSe}$ below 180 K, a new mid-infrared laser material *Opt. Lett.* **24** 1720–2
- [2] Mirov S B *et al* 2011 Progress in mid-IR Cr^{2+} and Fe^{2+} doped II–VI materials and lasers *Opt. Mater. Express* **1** 898–910
- [3] Kernal J *et al* 2005 3.9–4.8 μm gain-switched lasing of $\text{Fe}:\text{ZnSe}$ at room temperature *Opt. Express* **13** 10608–15
- [4] Velikanov S D *et al* 2015 Investigation of $\text{Fe}:\text{ZnSe}$ laser in pulsed and repetitively pulsed regimes *Quantum Electron.* **45** 1–7
- [5] Velikanov S D *et al* 2016 Room-temperature 1.2 J $\text{Fe}^{2+}:\text{ZnSe}$ laser *Quantum Electron.* **46** 11–12
- [6] Martyskhin D V *et al* 2015 High average power (35 W) pulsed $\text{Fe}:\text{ZnSe}$ laser tunable over 3.8–4.2 μm *Proc. of CLEO* (Optical Society of America) paper SF1F.2
- [7] Firsov K N *et al* 2016 Laser on single-crystal $\text{ZnSe}:\text{Fe}^{2+}$ with high pulse radiation energy at room temperature *Laser Phys. Lett.* **13** 015002
- [8] Firsov K N *et al* 2014 Spectral and temporal characteristics of a $\text{ZnSe}:\text{Fe}^{2+}$ laser pumped by a non-chain HF(DF) laser at room temperature *Laser Phys. Lett.* **11** 125004
- [9] Frolov M P *et al* 2013 Study of a 2 J pulsed $\text{Fe}:\text{ZnSe}$ 4 μm laser *Laser Phys. Lett.* **10** 125001
- [10] Firsov K N *et al* 2014 Increasing the radiation energy of $\text{ZnSe}:\text{Fe}^{2+}$ laser at room temperature *Laser Phys. Lett.* **11** 085001
- [11] Pan Q K *et al* 2016 Non-chain pulsed DF laser with an average power of the order of 100 W *Appl. Phys. B* **122** 200
- [12] Ruan P *et al* 2012 Computer modeling and experimental study of non-chain pulsed electric-discharge DF laser *Opt. Express* **20** 28912–22
- [13] Sennaroglu A, Konca A O and Pollock C R 2000 Continuous-wave power performance of a 2.47 μm $\text{Cr}^{2+}:\text{ZnSe}$ laser: experiment and modeling *IEEE J. Quantum Electron.* **36** 1199–205
- [14] Evans J W, Berry P A and Schepler K L 2012 840 mW continuous-wave $\text{Fe}:\text{ZnSe}$ laser operating at 4140 nm *Opt. Lett.* **37** 5021–3
- [15] Myoung N *et al* 2011 Energy scaling of 4.3 μm room temperature $\text{Fe}:\text{ZnSe}$ laser *Opt. Lett.* **36** 94–6
- [16] Fedorov V V *et al* 2006 3.77–5.05 μm tunable solid-state lasers based on Fe^{2+} -doped ZnSe crystals operating at low and room temperatures *IEEE J. Quantum Electron.* **42** 907–17
- [17] Cankaya H *et al* 2008 Absorption saturation analysis of $\text{Cr}^{2+}:\text{ZnSe}$ and $\text{Fe}^{2+}:\text{ZnSe}$ *J. Opt. Soc. Am. B* **25** 794–800